

Reversible data hiding in encrypted images based on pixel prediction and multi-MSB planes rearrangement

Zhaoxia Yin^a, Xiaomeng She^a, Jin Tang^{a,*}, Bin Luo^a

^a*Anhui Province Key Laboratory of Multimodal Cognitive Computation, School of Computer Science and Technology, Anhui University, 230601, P.R.China*

Abstract

Great concern has arisen in the field of reversible data hiding in encrypted images (RDHEI) due to the development of cloud storage and privacy protection. RDHEI is an effective technology that can embed additional data after image encryption, extract additional data error-free and reconstruct original images losslessly. In this paper, a high-capacity and fully reversible RDHEI method based on pixel prediction and multi-MSB (most significant bit) planes rearrangement is proposed. First, the median edge detector (MED) predictor is used to calculate the predicted value. Next, unlike previous methods, in our proposed method, signs of prediction errors (PEs) are represented by one bit plane and absolute values of PEs are represented by other bit planes. Then, we divide bit planes into uniform blocks and non-uniform blocks, and rearrange these blocks. Finally, according to different pixel prediction schemes, different number of additional data are embedded adaptively. The experimental results prove that our method has higher embedding capacity compared with state-of-the-art RDHEI methods.

Keywords: Reversible data hiding, encrypted images, privacy protection, prediction error

1. Introduction

Data hiding is a technique that can embed data into multi-media and extract the data error-free by modifying the cover medium slightly. In order to protect the cover medium, reversible data hiding (RDH) is proposed [1], which can reconstruct the cover medium losslessly. In the past several decades, RDH has attracted more and more attention, and has been applied in many fields, such as military communication, medical diagnosis, judicial evidence obtaining and so on [2].

A major current focus in RDH is how to ensure low distortion of original images after embedding data, therefore, visual quality of marked images is the key metric of RDH methods. To achieve better visual quality, many RDH methods have been proposed in the past several decades [3–13]. These methods are mainly divided into three categories: lossless compression [3–5], histogram shifting [6–10] and difference expansion [11–13]. The first category, lossless compression, is used in many RDH methods to vacate room for data embedding. To achieve better performance, lots of RDH methods based on histogram shifting have been proposed. The central idea of these methods is to use the peak points and minimum points of the histogram of an image, and embed additional data by modifying the grayscale values. The third category is based on difference expansion, which embeds data by expanding the difference between two pixels.

With the growing development of cloud storage and the ever-increasing demand for privacy protection, original images are typically encrypted before they are transmitted. Therefore,

reversible data hiding in encrypted images (RDHEI) methods [14–16] have attracted wide concern over the past years. As shown in Fig. 1, there are three end users of a RDHEI method: the content-owner, data-hider and receiver. The first end user, content-owner, is the original image provider, who has the right to access the original image and encrypt it. The second end user is the data-hider, who can only receive the encrypted image and embed additional data into the encrypted domain. Besides, the data-hider cannot access the content of original images. The final end user called receiver, he can restore the original image and extract the embedded data. Since the content of original images cannot be obtained after encryption, the visual quality of marked images don't need to be compared. Therefore, embedding capacity is the key metric of RDHEI rather than visual quality.

According to the encryption order, the existing RDHEI methods can be divided into two categories, Vacating Room After Encryption (VRAE) and Reserving Room Before Encryption (RRBE), as shown in Fig. 1. In VRAE methods [17–21], data-hiders embed additional data by modifying encrypted pixel values. However, because the entropy of encrypted images has been maximized, VRAE methods can only achieve low embedding capacity. To further improve embedding capacity, many RRBE methods have been proposed in the past few years [22–28]. Different from VRAE methods, these methods improve embedding capacity based on the spatial correlation of original images. In this paper, we focus on RRBE methods.

In [22], Ma et al. first proposed the RRBE scheme. The key idea of their scheme is to reserve room by embedding the least significant bit (LSB) of some original pixels into other original pixels. Then generate an encrypted image and embed addi-

*Corresponding author

Email address: tangjin@ahu.edu.cn (Jin Tang)

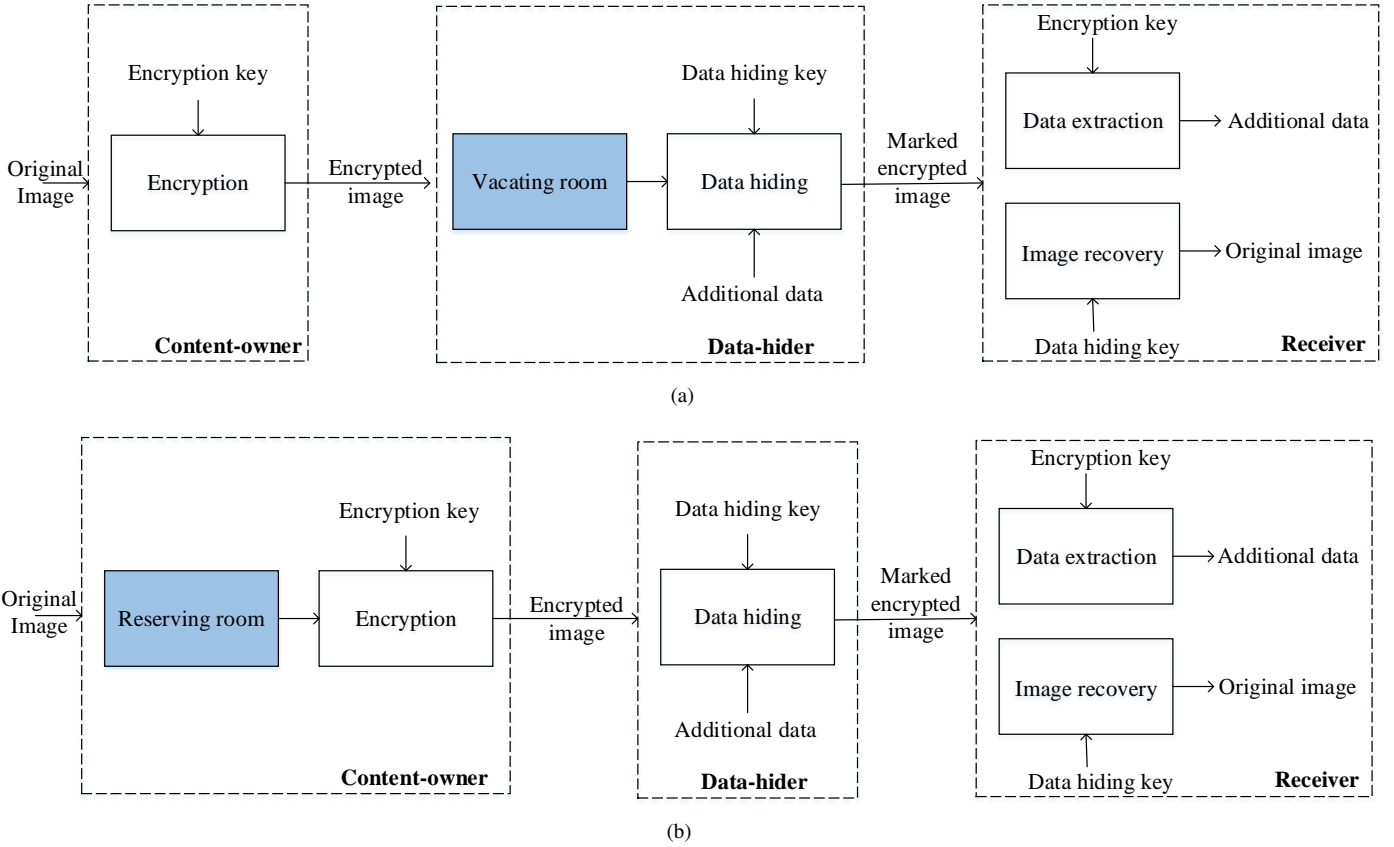


Figure 1: Two categorized frameworks of RDHEI schemes: (a) VRAE and (b) RRBE.

tional data into the reserved room. In comparison with previous VRAE schemes, this scheme further improves the embedding capacity, and hence makes RRBE scheme viable. Yi et al. [23] suggested embedding the lower bit planes of original images into the higher bit planes so that the room of lower bit planes can be used to embedding data. In the early work, most of ways to increase embedding capacity of RDHEI was to research regarding the LSB substitution, and little attention was paid to the substitution of MSB. Puteaux et al. [24] proposed a new RDHEI scheme based on MSB substitution instead of LSB, which can achieve higher capacity than previous schemes. They designed a MSB prediction scheme, and generated a label map from which data can be embedded. However, one point of this scheme can be improved is that only one-MSB can be used. Based on [24], Puyang et al. [25] proposed an extension scheme using two-MSB prediction, which is more efficient and the performance is improved. Later, Yin et al. [26] also proposed an improved scheme based on [25]. During their reserving embeddable room phase, multi-MSB of original pixels are predicted adaptively and marked by Huffman coding. According to their results, the embedding capacity is higher than previous methods. In [27], Wu et al. suggested taking advantage of the spatial correlation of original images and using parametric binary tree labeling to mark image pixels in two different categories. By using this scheme, original images can be recovered losslessly and embedding capacity can also be improved. Ren et al. [28]

proposed a RDH scheme for encrypted binary images, which takes advantage of the point that binary images have only two kinds of pixels. Then, additional data is embedded into pixel blocks based on the spatial correlation in this scheme.

Although the RDHEI methods mentioned above have achieved relatively good performance, high embedding capacity or full reversibility has not been achieved. Hence, these methods are not satisfactory enough. For example, since Puteaux et al.'s method [24] is limited to MSB and other bits are not fully utilized, the embedding capacity is far from satisfaction. Then, although Yin et al. [26] have taken into account multiple MSBs, their method generates a lot of auxiliary data. The auxiliary data cannot be compressed well and takes too much room, which makes the net payload of this method not high enough. Wu et al. [27] proposed to mark pixels with a parameter binary tree and divide them into two categories, which would make some pixels unable to embed data and affect the performance of embedding capacity. Considering the similarity between bit planes of grayscale images and binary images, that is, both bit planes and binary images are only composed of two types of values. Ren et al.'s scheme [28] was directly applied to grayscale images by us, however, the embedding capacity is not satisfactory when this application is reversible. There are two main reasons for the limited embedding capacity: In the application, the bit planes of original images don't have enough room to accommodate additional data compared with the prediction error

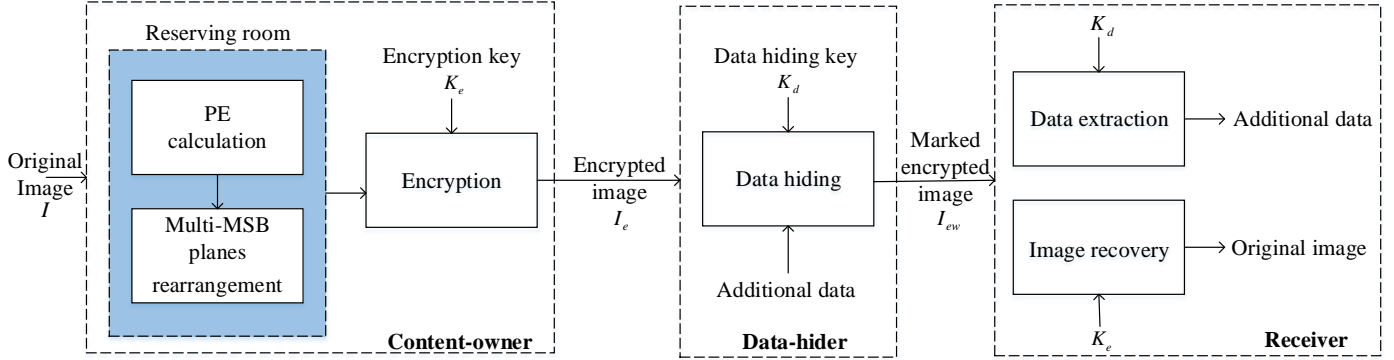


Figure 2: The framework of the proposed method.

(PE) bit planes in our paper; This application will generate too much auxiliary data without significant sparse features, hence it cannot be well compressed. To achieve better performance, in this paper, we propose a new method which effectively reduces these unsatisfactory points.

The main contributions of our method can be summarized as follows:

1) We successfully extend the pixel prediction scheme of binary image to bit planes of grayscale image, and solve the problem that high embedding capacity and reversibility cannot coexist. In a word, after we improve the embedding capacity, our method is still reversible.

2) We make full use of the correlation of adjacent pixels and compress auxiliary data with sparse features via arithmetic coding, which makes more embeddable positions in the bit planes. Experimental results also prove that we have achieved a higher embedding capacity compared with the most advanced RDHEI method.

3) Furthermore, we have successfully used the median edge predictor (MED). The distribution of PE values becomes smaller relative to the distribution range of original pixel values, which exploits spatial redundancy better and makes the available embedded room larger.

The rest of this paper is organized as follows: The proposed method is described in detail in Section 2, and Section 3 introduces the experimental results and analysis of our method. Finally, this paper is concluded in Section 4.

2. Proposed method

In this section, we propose a high-capacity and fully reversible RDHEI method based on pixel prediction and multi-MSB planes rearrangement. As shown in Fig. 2, the proposed method can be divided into three parts: 1) Embeddable room reservation and encryption are done by content-owner, 2) Data embedding is done by data-hider, 3) Data extraction and image recovery are done by receiver. In this section, the proposed method is introduced in detail. First, Section 2.1 describes the process of reserving embeddable room. Next, in Section 2.2, procedures of image encryption are given. Then, Section 2.3 presents the process of additional data embedding. In the last

Section 2.4, data extraction and image recovery are described in detail.

2.1. Embeddable room reservation

The procedures of this section are divided into three parts: Calculation of predicted errors, generation of bit planes and rearrangement of bit planes.

2.1.1. Calculation of prediction errors

For an original image I sized $M \times N$, predicted value px is calculated by the MED predictor [29]. As shown in Fig. 3, px is calculated based on the three pixels around the current pixel x . In particular, the pixels of first row and first column will be the reference pixels to recover original image, hence the value of them will not be changed.

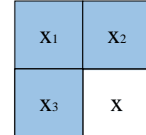


Figure 3: The context of the current pixel by MED predictor.

The detailed calculation formula of predicted values is as follows:

$$px = \begin{cases} \max(x_2, x_3) & , \quad x_1 \leq \min(x_2, x_3) \\ \min(x_2, x_3) & , \quad x_1 \geq \max(x_2, x_3) \\ x_2 + x_3 - x_1 & , \quad \text{otherwise} \end{cases} \quad (1)$$

Then, the PE $e(i, j)$ can be obtained as follows:

$$e(i, j) = \begin{cases} x(i, j) & , \quad i = 1 \text{ or } j = 1 \\ x(i, j) - px(i, j) & , \quad \text{otherwise} \end{cases} \quad (2)$$

where $1 \leq i \leq M, 1 \leq j \leq N$.

Finally, we define $e(i, j)$ greater than 64 or less than -64 as overflow pixels, and use Eq. (3) to change the value of these pixels. The reason for this operation will be explained later. After the calculation, the distribution of PEs is more concentrated than that of the original pixel values, which means that

there are more identical values in bit planes and the embedding capacity will be improved.

$$e(i, j) = x(i, j) \quad , \quad e(i, j) < -64 \text{ or } e(i, j) > 64. \quad (3)$$

2.1.2. Generation of bit planes

After calculating the PEs, the PE bit planes are generated. If only traditional method, Eq. (4), is used to calculate bit planes, the proposed scheme will not be reversible. Since the original positions of bit planes are shuffled in the subsequent embedding operation, whether the PE is positive or negative during the image recovery step cannot be determined. Based on this problem, an adaptive method is proposed to calculate PE bit-planes by us. The method is introduced in detail as follows: First, considering the range of pixel values of grayscale images, the PEs of reference pixels are converted into 8-bit binary sequences by Eq. (4), where $i=1$ or $j=1$ and $\lfloor \cdot \rfloor$ is the floor operations.

$$e^k(i, j) = \left\lfloor \frac{e(i, j) \bmod 2^{9-k}}{2^{8-k}} \right\rfloor, k = 1, 2, \dots, 8. \quad (4)$$

Next, other PEs are converted into 7-bit binary sequences by Eq. (5). What's more, since there are some overflow PEs, we use Eq. (6) to calculate the eighth binary bit of PEs in different situations. Specifically, signs of non-overflow PEs are represented by one bit plane and absolute values of non-overflow PEs are represented by other bit planes. However, although PEs are converted into 7-bit binary sequences, the final reconstructed image is still lossless, because only a few PE values are overflow values (the PE values less than -64 or greater than 64 are overflow PEs). The calculation formulas for this step are as follows:

$$e^k(i, j) = \left\lfloor \frac{e(i, j) \bmod 2^{9-k}}{2^{8-k}} \right\rfloor, k = 1, 2, \dots, 7, \quad (5)$$

$$e^8(i, j) = \begin{cases} 1 - \text{sign } e(i, j) & , \quad -64 \leq e(i, j) \leq 64 \\ e(i, j) \bmod 2 & , \quad \text{otherwise} \end{cases}. \quad (6)$$

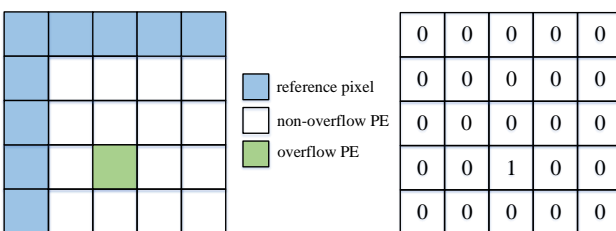


Figure 4: The label map of PE image.

Finally, because we use different formulas to convert PEs, a PE label map must be generated to identify each PE. Thus, we set the tag 1 for overflow PEs and 0 for other PEs. In this way, a label map L_1 with a large number of 0 and a fairly small number of 1 is generated. Besides, arithmetic coding is used to compress L_1 losslessly. Particularly, the compressed auxiliary data only occupies a very small room. For better understanding, as shown in Fig. 4, an example is given to describe our method.

2.1.3. Rearrangement of bit planes

First, as shown in Fig. 5, the bit planes obtained by the above steps are divided into several non-overlapping blocks sized $k \times k$. All values are the same for uniform blocks (UB), otherwise they are non-uniform blocks (NUB). Since there are much redundancy in the multi-MSB planes, the number of UB is much larger than that of NUB. Similarly, NUB and UB are labeled by 1 and 0 respectively. The label map L_2 with sparse feature can be obtained and well compressed, and the length of the map is expressed in a 16-bit binary sequence. Then, the processed bit planes are traversed in order, the NUBs of each bit plane are arranged in order in the upper order, and the UBs in the lower order, as shown in Fig. 6. Meanwhile, all of NUBs need to be marked, and the NUB that can be embedded into additional data is marked with 0, otherwise 1. The specific basis for judging whether NUB can be embedded will be mentioned later.

0	1
0	0

Figure 5: An example of original blocks labeling of bit planes.

NUB	UB
UB	UB

Figure 6: Rearrangement of bit planes.

Lastly, we embed all the auxiliary data into UBs of the corresponding bit plane, and the last value of each UB is used as the predicted value without auxiliary data. Moreover, since some bit planes are not enough to accommodate auxiliary data, an 8-bit binary sequence is finally generated to indicate whether the current bit plane can be embedded.

2.2. Generation of the encrypted image

After reserving the embeddable room, the next step is to encrypt the image. First, the image is divided into eight bit planes, and the auxiliary data is extracted sequentially in the lower right of each bit plane in order to locate the encrypted position. Next, a pseudo-random matrix H of size $M \times N$ is generated by an encryption key K_e , the values of this matrix are converted into 8-bit binary sequences by Eq. (7),

$$H^k(i, j) = \left\lfloor \frac{H(i, j) \bmod 2^{9-k}}{2^{8-k}} \right\rfloor, k = 1, 2, \dots, 8, \quad (7)$$

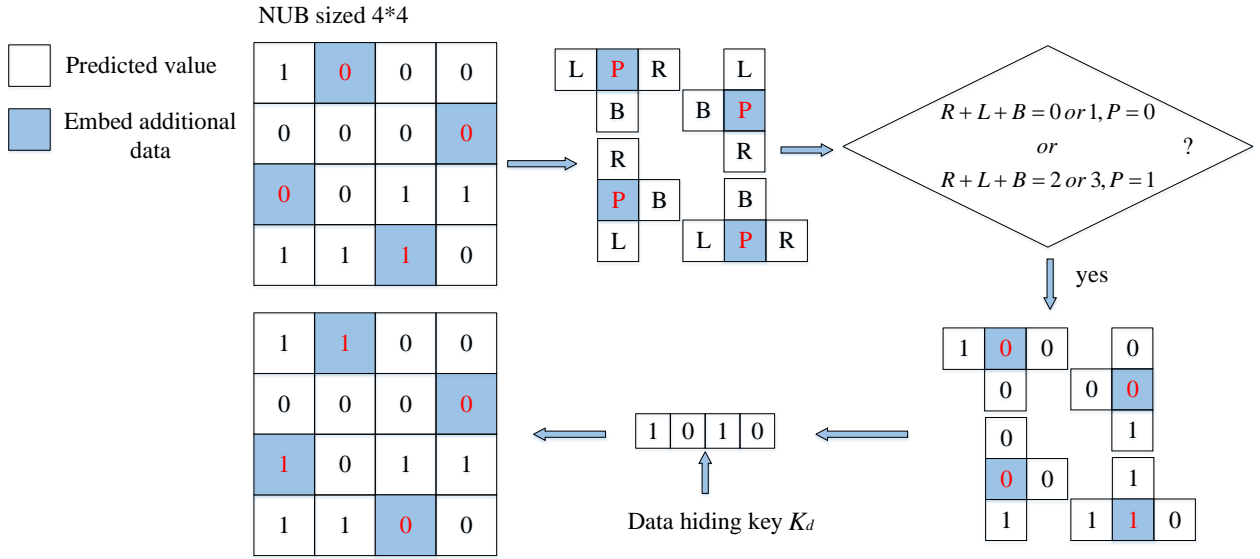


Figure 7: An example of embedding data into NUB.

where $1 \leq i \leq M, 1 \leq j \leq N$. At last, for the original PE $e^k(i, j)$ of each bit plane that can be encrypted, we use the Eq. (8) to perform encryption operations and \oplus denotes exclusive-or (XOR) operation:

$$e_e^k(i, j) = e^k(i, j) \oplus H^k(i, j), \quad k = 1, 2, \dots, 8. \quad (8)$$

In this way, we can calculate the encrypted PE $e_e^k(i, j)$ of k^{th} bit plane and finally get the encrypted image I_e .

2.3. Generation of the marked encrypted image

Considering the similarity between bit planes and binary images, we use the pixel prediction scheme when embedding additional data into the processed PE bit planes, which is proposed by Ren et al. [28]. As mentioned before, each processed bit plane is divided into UBS and NUBs. For different blocks, different methods are used to embed additional data. Besides, to improve the security of our method, the data hiding key K_d is used to encrypt additional data before embedding. After completing these steps, embedding steps are described in detail below.

First, we embed additional data into NUBs. Auxiliary data in the lower right corner of the MSB plane needs to be extracted first to determine whether each bit plane can be embedded and the embedded coordinates. It can be seen from pixel correlation that the probability of adjacent pixels being identical is very high. However, values of bit planes are only 0 and 1, which means that the probability of three adjacent values around each value being identical is very high. For each NUB, if the value of middle position is 0, the sum of three neighboring values may be 0 or 1 (that is, the probability of neighboring values being 0 is higher than 1). Similarly, if the middle value is 1, the sum of three neighboring values may be 2 or 3. Based on this feature, we judge each NUB, if current NUB satisfies the feature, it is an embeddable block. Conversely, additional data cannot be embedded. As shown in Fig. 7 is an example of embedding

data into NUB. Each NUB is divided into four parts, and each part is composed of four values, where P is the middle position of each part that can be embedded, and L, B, R are the three adjacent predicted values around P .

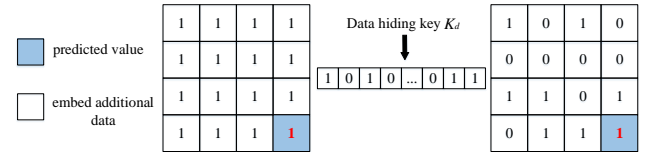


Figure 8: An example of embedding data into UB.

Then, we embed data into UBS. According to the extracted auxiliary data, the embeddable coordinates in UB can be easily located. As shown in Fig. 8, for each UB, the values of one block are identical. This means that, for a UB, we only need to keep one of value in the block not being changed, and then we can recover all values in the block after taking the unchanged value as the prediction value. Based on this characteristic, we embed additional data into UBS except the position of predicted value. To facilitate understanding, here is an example of embedding data into a UB. As shown in Fig. 8 is a UB that each value is 1. After we embed data, only the last value 1 remains unchanged. Finally, after embedding additional data into NUBs and UBSs, we have generated the marked encrypted image I_{ew} .

2.4. Data extraction and image recovery

Whether the receiver obtains the embedded data or the original image depends on which key the receiver has. Therefore, three cases are given according to the different keys owned by the receiver:

1) If the receiver has the data hiding key K_d , the embedded data can be obtained without errors. First, the legal receiver divides the marked encrypted image into eight bit planes according to the auxiliary data in the lower right corner of the

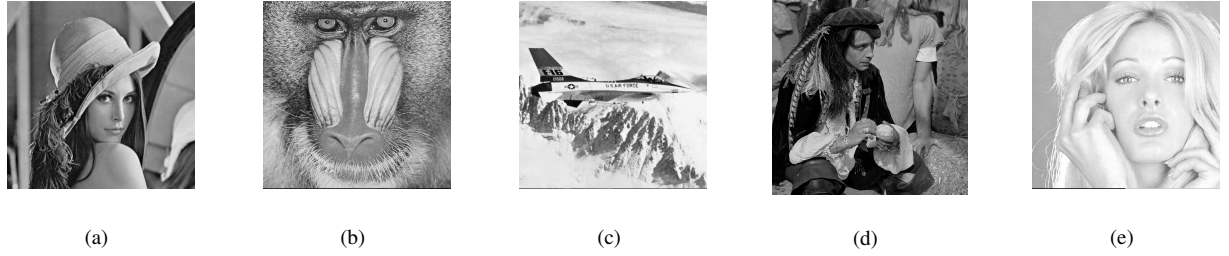


Figure 9: Test images: (a) *Lena*; (b) *Baboon*; (c) *Jetplane*; (d) *Man*; (e) *Tiffany*.

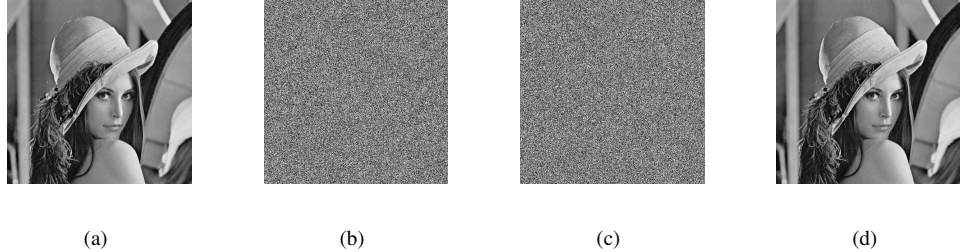


Figure 10: Results of applying our method to *Lena* image when $k=4$: (a) Original image I ; (b) Encrypted image I_e ; (c) Marked encrypted image I_{ew} , with net payload ER = 2.87 bpp; (d) Reconstructed image I .

MSB plane. If the current bit plane is an embeddable bit plane, locate the position where the additional data is embedded, and then extract auxiliary data of remaining embeddable bit planes in sequence. For each NUB, if the auxiliary data of this NUB is 0, additional data can be extracted in this NUB. For each UB, except for the prediction pixel of the last position, the additional data of other positions is extracted in order. Finally, all embedded additional data can be extracted without errors and decrypted with the data hiding key K_d . Since the receiver does not have the encryption key K_e , the original image cannot be recovered.

2) If the receiver has the encryption key K_e , the original image can be reconstructed losslessly. First, the legal receiver decrypts the marked encrypted image with the encryption key K_e , and extracts auxiliary data in the lower right corner of the MSB plane to determine whether each bit plane is rearranged. Then, the auxiliary data of remaining bit planes is sequentially extracted. According to the prediction scheme mentioned above, all of NUBs and UBs in embeddable bit planes can be restored. Finally, according to the extracted label map L_2 , the receiver can reconstruct the original image losslessly.

3) If the receiver has both the data hiding key K_d and the encryption key K_e , then the data can be extracted error-free and images can be recovered losslessly. The detailed steps are the same as above.

3. Experimental results and analysis

To clearly evaluate the performance of our proposed scheme, experimental results and analysis are detailed in this section. First, several experimental results are summarized in Section 3.1. As shown in Fig. 9, five commonly used test images *Lena*, *Baboon*, *Jetplane*, *Man* and *Tiffany* are used as examples to

show the experimental results. Furthermore, we also realize tests on three public datasets: BOSSbase [30], BOWS-2 [31] and UCID [32]. Then, Section 3.2 gives performance analysis in terms of reversibility and embedding capacity. Finally, Section 3.3 compares the proposed method with recent state-of-the-art methods.

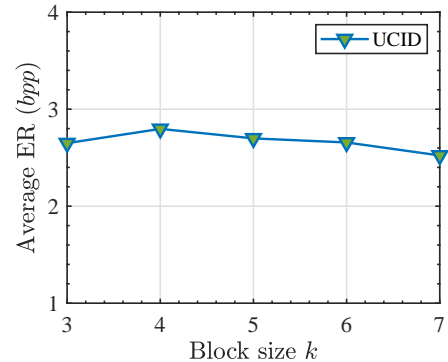


Figure 11: The average ERs of test images in dataset UCID [32] when block size k is different.

3.1. Experimental results

Fig. 10 shows the experimental results of applying our method to *Lena* image when block size $k=4$. The original *Lena* image I is presented in Fig. 10(a). After the content-owner completes the steps of reserving room and encryption, the encrypted image I_e in Fig. 10(b) can be obtained. Then, the data-hider embeds additional data into the encrypted image I_e and generates a marked encrypted image I_{ew} in Fig. 10(c). It can be clearly seen that without the key, the content of the original image cannot be

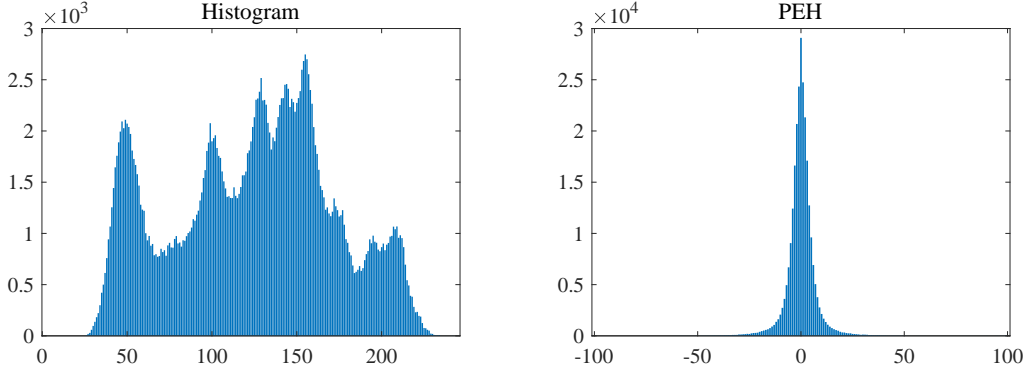


Figure 12: Original image histogram and prediction error histogram (PEH).

obtained by unauthorized users only from the encrypted image I_e or the marked encrypted image I_{ew} , and both of images have security from the analysis in [33]. Fig. 10(d) displays the recovered *Lena* image, visual quality and MSE (Mean square error) equal to 0 prove that the recovered *Lena* image is exactly the same as the original *Lena* image. Since the size of embedding capacity is the key metric of RDHEI, we use the embedding rate (ER) as the evaluation index of embedding capacity. In addition, because we divided bit planes into several non-overlapping blocks sized $k \times k$ and k is a variable, in Fig. 11, we give the experimental results when block sizes are different on public dataset UCID [32]. Compared with other block sizes, ER is the highest when the block size k is 4, so our experiments are completed when k is 4. Table. 1 shows the test results on three public datasets: BOSSbase [30], BOWS-2 [31] and UCID [32]. The average ERs are 3.498 *bpp* (bits per pixel), 3.393 *bpp* and 2.797 *bpp* respectively when block size $k=4$. Moreover, the MSE of the recovered images on three datasets are 0, which indicates that each recovered image is exactly identical with the corresponding original image. In conclusion, RDHEI scheme can be perfectly achieved by our proposed method.

3.2. Performance analysis

In this section, we analyze the performance of proposed method according to the contributions mentioned earlier. The first is about reversibility. It can be seen from Table. 1 that after using the proposed method, the MSE of the restored image on the three datasets is all 0. It means that our method is fully reversible. Next is the analysis on embedding capacity, which is the key indicator of RDHEI. As talked in the previous sections, the pixel prediction scheme of binary images can be directly applied to the bit plane of grayscale images, but experimental results demonstrate the embedding capacity is unsatisfactory. However, our method can achieve high embedding capacity.

One of the reasons is that our method doesn't generate too much auxiliary data to occupy many embeddable room, and the auxiliary data can be perfectly compressed. As mentioned in Section 2.1, the auxiliary data in this paper is mainly composed of L_1 and L_2 . L_1 is the label map of overflow pixels and total pixels, and the original size is the same as the original image. However, the percentage of overflow pixels and total pixels is

Table 1: Experimental results on three image databases.

Database	MSE	Average ER(<i>bpp</i>)
BOSSbase	0	3.498
BOWS-2	0	3.393
UCID	0	2.797

extremely low. For example, in the five commonly used images, the percentages are 0.04%, 1.42%, 0.16%, 0.09% and 0.02% respectively. Thus, we set tag 1 for overflow pixels, 0 for other pixels, and L_1 with a large number of 0 and a few 1 is generated. It can be perfectly compressed by arithmetic coding because the sequence L_1 is sparse. L_2 is another label map, which shows the original positions of UBS and NUBs before the bit plane is rearranged. Since there are more UBS and less NUBs in most PE bit planes, we also set tag 1 for NUBs, 0 for UBS to generate L_2 . In the same way, arithmetic coding can be used to compress L_2 . After compression, there is more room in bit planes to embed additional data, which further improves the ER of our method.

Another reason is that we reserve the room of PE bit planes instead of the original bit planes. In the proposed method, we use the MED predictor to calculate predicted values. After the calculation, as shown in Fig. 12, the distribution of PEs is more concentrated than that of original pixel values. In other words, it makes more values in bit planes being identical and means that more data can be embedded into UBS. In summary, the proposed method exploits spatial redundancy better and makes the available embedded room larger, hence the performance of it is more satisfactory.

3.3. Comparison with state-of-the-art methods

To better verify the good performance of the proposed method, this section compares ER with three latest state-of-the-art RDHEI methods [24, 26, 27]. As shown in Figure. 13, five commonly used images are tested by using these methods, and it can be seen that our method outperforms the other three methods with highest ER.

Different from our method of embedding data into multiple MSBs, Puteaux et al. [24] only embedded data into the MSB, and other bits are not fully utilized. Hence the ER of

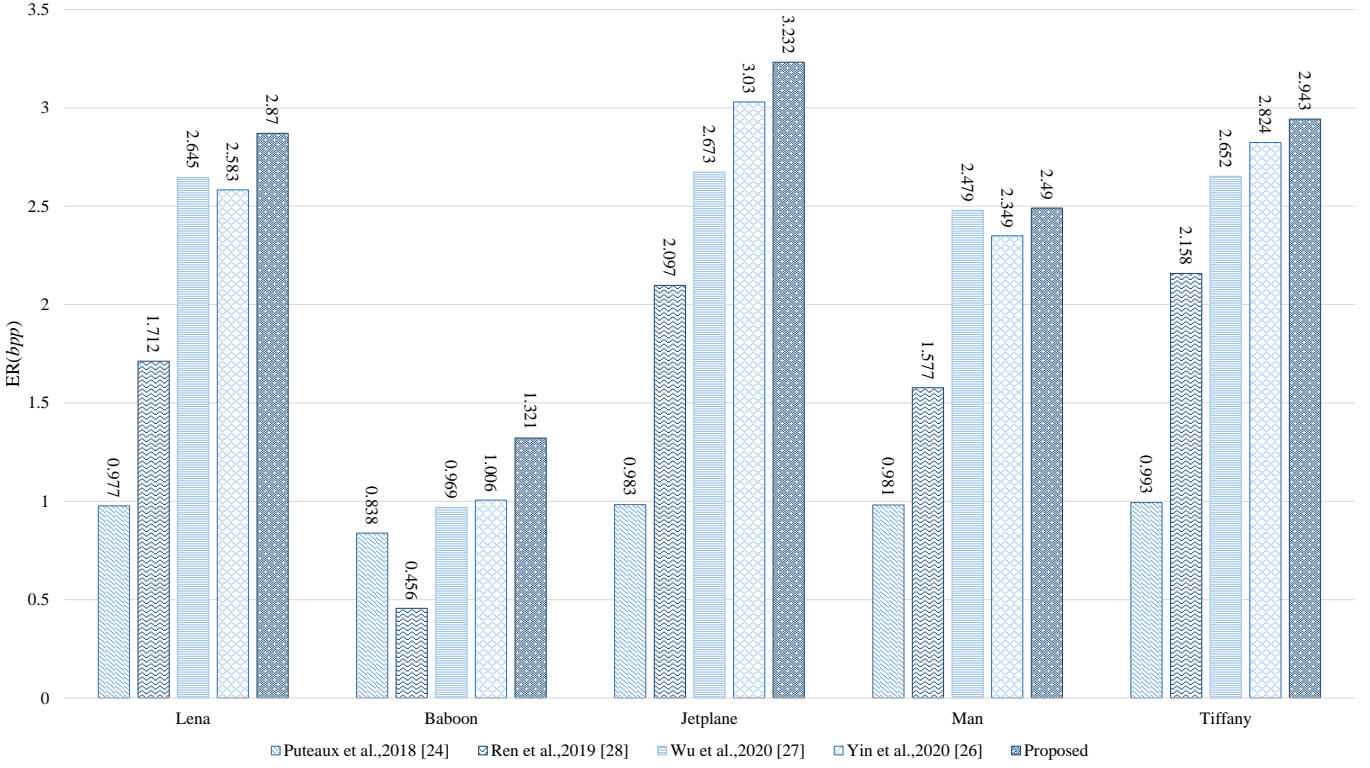


Figure 13: Comparison of ER (bpp) on five test images.

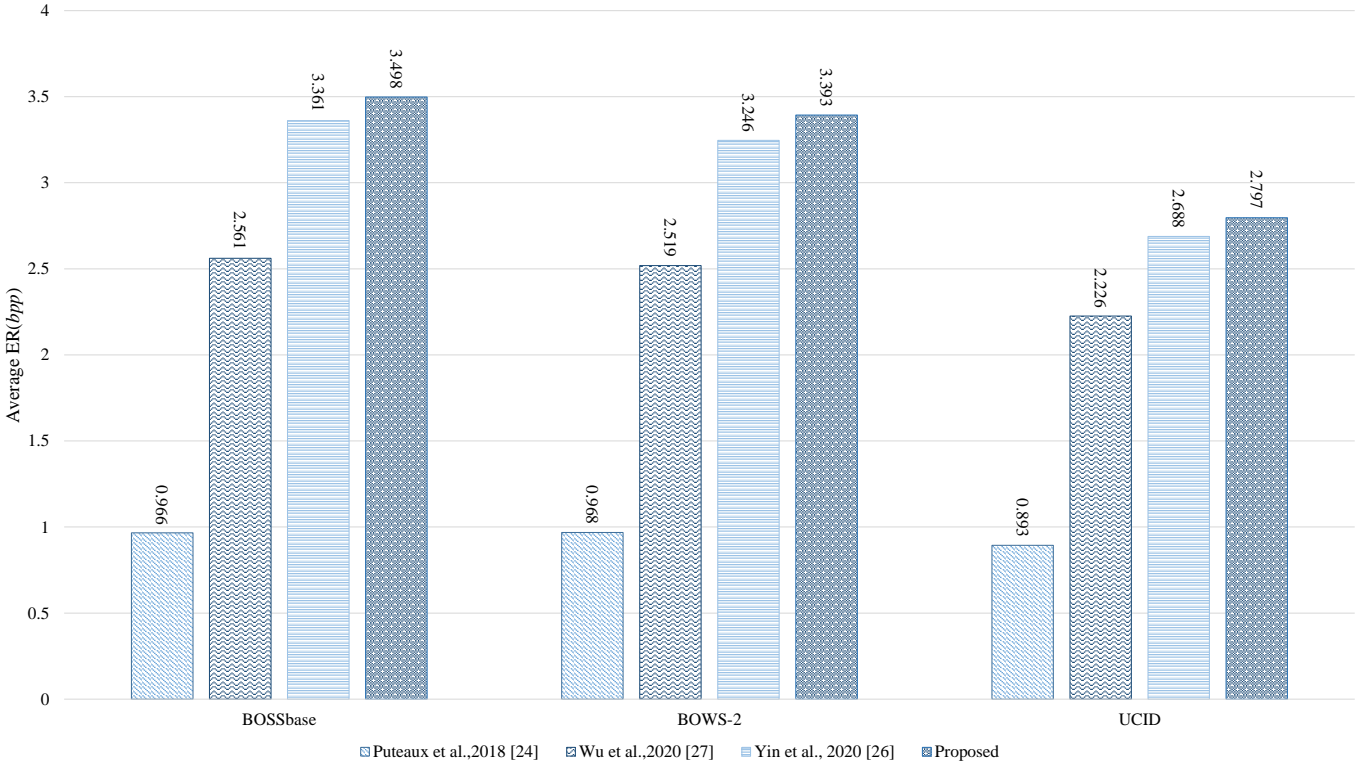


Figure 14: Average ER (bpp) comparison in different datasets BOSSBase [30], BOWS-2 [31], and UCID [32].

their method is very low. For example, in [24], the ERs of five commonly used images are only 0.977 bpp , 0.838 bpp , 0.983

bpp , 0.981 bpp and 0.993 bpp . In [27], Wu et al. suggested marking pixels with a parameter binary tree and dividing them

into two categories, which would make some pixels unable to embed additional data and affect the performance of embedding capacity. The ERs of five test images in their paper are 2.645 bpp , 0.969 bpp , 2.673 bpp , 2.479 bpp and 2.652 bpp . In addition, Yin et al. [26] uses multiple MSBs, but the auxiliary data generated by this method is very large and cannot be compressed well, so the embeddable room of each bit plane is still not well utilized. When using the method of Yin et al. [26], the ERs of five test images are 2.583 bpp , 1.006 bpp , 3.03 bpp , 2.349 bpp and 2.824 bpp . However, the experimental results of five images in this paper are 2.87 bpp , 1.321 bpp , 3.232 bpp , 2.49 bpp , 2.943 bpp respectively, which are higher than previous methods. Finally, to better prove the performance of our method, we have directly applied the binary image method of Ren et al. [28] to grayscale images. This method performs reversing operations directly on original bit planes. Since there are only a few embeddable positions in original bit planes compared to the prediction error bit planes proposed in our paper, the embedding capacity is unsatisfactory. Furthermore, this method will generate too much auxiliary data, which is not sparse sufficiently. Therefore, the auxiliary data cannot be well compressed and direct application will not achieve high embedding capacity. In other word, direct application can only achieve high embedding capacity without embedding auxiliary data. However, it is impossible to realize reversibility without embedding auxiliary data. On the contrary, if we want to achieve reversibility, the embedded capacity cannot be satisfactory. Our experimental results show that, as mentioned in the previous contributions, we have solved the problem that high embedding capacity and reversibility cannot coexist. Taking the *Lena* image as an example, as shown in Figure. 13, the ER is only 1.712 bpp . It is worth mentioning that the ER of *Lena* image when using our method is 2.87 bpp . At last, we also compared the ER with these state-of-the-art methods on three datasets: BOSSbase [30], BOWS-2 [31] and UCID [32]. As shown in Figure. 14, it is obvious that the proposed method has a higher ER on these datasets than other methods.

4. Conclusions

This paper proposes a new method of reversible data hiding in encrypted images based on pixel prediction scheme and multi-MSB planes rearrangement, which achieves a higher embedding capacity compared with previous methods. It is worth noting that compared with previous methods, we can make better use of the correlation of adjacent pixels. The experimental results show that our method not only has a significantly increase in net payload, but also has reversibility. It's also worth mentioning that our method achieves higher ER than using pixel prediction scheme directly on grayscale images. Main reasons for better performance are: First, the distribution of prediction errors is more concentrated than that of original pixel values, and more embeddable positions of the bit plane can be used to embed data. Next, we mark the auxiliary data more effectively. According to the characteristics of the mark, we can compress it effectively by arithmetic coding, which makes more space available.

In the future work, we will continue to work on improving the performance of our algorithm. For example, we can reduce the number of auxiliary data as much as possible, and use more accurate prediction schemes to improve embedding rate. In addition, we hope that this paper will enable readers to understand the possibility of applying binary image algorithm to grayscale images, and the idea of improving performance during application. In the future, it is very practical to explore more general algorithms based on binary images and grayscale images.

Acknowledgments

This research work is partly supported by National Natural Science Foundation of China (61872003, U1636206 and 61860206004).

References

- [1] J. M. Barton, Method and apparatus for embedding authentication information within digital data, uS Patent 5,646,997 (1997).
- [2] Y.-Q. Shi, X. Li, X. Zhang, H.-T. Wu, B. Ma, Reversible data hiding: advances in the past two decades, *IEEE access* 4 (2016) 3210–3237.
- [3] M. U. Celik, G. Sharma, A. M. Tekalp, E. Saber, Lossless generalized-lsb data embedding, *IEEE transactions on image processing* 14 (2) (2005) 253–266.
- [4] M. U. Celik, G. Sharma, A. M. Tekalp, Lossless watermarking for image authentication: a new framework and an implementation, *IEEE Transactions on Image Processing* 15 (4) (2006) 1042–1049.
- [5] W. Zhang, X. Hu, X. Li, N. Yu, Recursive histogram modification: establishing equivalency between reversible data hiding and lossless data compression, *IEEE transactions on image processing* 22 (7) (2013) 2775–2785.
- [6] Z. Ni, Y.-Q. Shi, N. Ansari, W. Su, Reversible data hiding, *IEEE Transactions on circuits and systems for video technology* 16 (3) (2006) 354–362.
- [7] X. Li, B. Li, B. Yang, T. Zeng, General framework to histogram-shifting-based reversible data hiding, *IEEE Transactions on image processing* 22 (6) (2013) 2181–2191.
- [8] Y. Jia, Z. Yin, X. Zhang, Y. Luo, Reversible data hiding based on reducing invalid shifting of pixels in histogram shifting, *Signal Processing* 163 (2019) 238–246.
- [9] B. Ou, Y. Zhao, High capacity reversible data hiding based on multiple histograms modification, *IEEE Transactions on Circuits and Systems for Video Technology*.
- [10] X. Gao, Z. Pan, E. Gao, G. Fan, Reversible data hiding for high dynamic range images using two-dimensional prediction-error histogram of the second time prediction, *Signal Processing* 163 (2020) 107579.
- [11] J. Tian, Reversible data embedding using a difference expansion, *IEEE transactions on circuits and systems for video technology* 13 (8) (2003) 890–896.
- [12] A. M. Alattar, Reversible watermark using the difference expansion of a generalized integer transform, *IEEE transactions on image processing* 13 (8) (2004) 1147–1156.
- [13] H. J. Kim, V. Sachnev, Y. Q. Shi, J. Nam, H.-G. Choo, A novel difference expansion transform for reversible data embedding, *IEEE Transactions on Information Forensics and Security* 3 (3) (2008) 456–465.
- [14] W. Puech, M. Chaumont, O. Strauss, A reversible data hiding method for encrypted images, in: *Security, Forensics, Steganography, and Watermarking of Multimedia Contents X*, Vol. 6819, International Society for Optics and Photonics, 2008, p. 68191E.
- [15] W. Zhang, K. Ma, N. Yu, Reversibility improved data hiding in encrypted images, *Signal Processing* 94 (2014) 118–127.
- [16] D. Xu, R. Wang, Separable and error-free reversible data hiding in encrypted images, *Signal Processing* 123 (2016) 9–21.
- [17] X. Zhang, Reversible data hiding in encrypted image, *IEEE signal processing letters* 18 (4) (2011) 255–258.
- [18] X. Zhang, Separable reversible data hiding in encrypted image, *IEEE transactions on information forensics and security* 7 (2) (2011) 826–832.

- [19] W. Hong, T.-S. Chen, H.-Y. Wu, An improved reversible data hiding in encrypted images using side match, *IEEE Signal Processing Letters* 19 (4) (2012) 199–202.
- [20] X. Wu, W. Sun, High-capacity reversible data hiding in encrypted images by prediction error, *Signal processing* 104 (2014) 387–400.
- [21] Z. Yin, B. Luo, W. Hong, Separable and error-free reversible data hiding in encrypted image with high payload, *The scientific world journal* 2014.
- [22] K. Ma, W. Zhang, X. Zhao, N. Yu, F. Li, Reversible data hiding in encrypted images by reserving room before encryption, *IEEE Transactions on information forensics and security* 8 (3) (2013) 553–562.
- [23] S. Yi, Y. Zhou, Binary-block embedding for reversible data hiding in encrypted images, *Signal Processing* 133 (2017) 40–51.
- [24] P. Puteaux, W. Puech, An efficient msb prediction-based method for high-capacity reversible data hiding in encrypted images, *IEEE Transactions on Information Forensics and Security* 13 (7) (2018) 1670–1681.
- [25] Y. Puyang, Z. Yin, Z. Qian, Reversible data hiding in encrypted images with two-msb prediction, in: 2018 IEEE International Workshop on Information Forensics and Security (WIFS), IEEE, 2018, pp. 1–7.
- [26] Z. Yin, Y. Xiang, X. Zhang, Reversible data hiding in encrypted images based on multi-msb prediction and huffman coding, *IEEE Transactions on Multimedia* 22 (4) (2020) 874–884.
- [27] Y. Wu, Y. Xiang, Y. Guo, J. Tang, Z. Yin, An improved reversible data hiding in encrypted images using parametric binary tree labeling, *IEEE Transactions on Multimedia* 22 (8) (2020) 1929–1938.
- [28] H. Ren, W. Lu, B. Chen, Reversible data hiding in encrypted binary images by pixel prediction, *Signal Processing* 165 (2019) 268–277.
- [29] M. J. Weinberger, G. Seroussi, G. Sapiro, The loco-i lossless image compression algorithm: Principles and standardization into jpeg-ls, *IEEE Transactions on Image processing* 9 (8) (2000) 1309–1324.
- [30] P. Bas, T. Filler, T. Pevný, "break our steganographic system": the ins and outs of organizing boss, in: International workshop on information hiding, Springer, 2011, pp. 59–70.
- [31] P. Bas, T. Furun, Image database of bows-2, Accessed: Jun 20.
- [32] G. Schaefer, M. Stich, Ucid: An uncompressed color image database, in: Storage and Retrieval Methods and Applications for Multimedia 2004, Vol. 5307, International Society for Optics and Photonics, 2003, pp. 472–480.
- [33] C. Li, Y. Zhang, E. Y. Xie, When an attacker meets a cipher-image in 2018: A year in review, *Journal of Information Security and Applications* 48 (2019) 102361.